

*Dedicated to the memory of Prof. dr. Ioan Silaghi-Dumitrescu marking 60 years from his birth*

## ON THE MULTIPLE FACETS OF AROMATICITY: ORGANIC, INORGANIC, ORGANOMETALLIC, COORDINATION AND SUPRAMOLECULAR CASE STUDIES

MARILENA FERBINTEANU<sup>a</sup>, FANICA CIMPOESU<sup>b</sup>

**ABSTRACT.** This work is an original synopsis over different structural patterns, from different areas of chemistry, unified under the broadened paradigm of the aromaticity. Cluster, coordination and supramolecular systems selected from our own work, as well as correlated literature examples are gathered together and revisited with state of the art electron structure methods and post-computational analyses. Methodological innovations, such as the vibronic approach and the simulation of resonance structures by enforced electron population of correspondingly prepared natural bond orbitals afforded the revealing of new keys for the old keyword of aromaticity.

**Keywords:** *aromaticity, ab initio calculations, vibronic models, resonance structures, natural bond orbitals, coordination chemistry, organometallic chemistry, supramolecular assembling.*

### INTRODUCTION

The aromaticity [1,2] concept is a perennial asset in the heuristic panoply of chemistry, a valuable currency for exchanging ideas between experimental and theoretical sides of communities exploring structure-property correlations, in both fundamental and application respects. Aside the usefulness of the term for taxonomy and reactivity thumb rules in the organic chemistry, [3] its relevance goes up to the advanced material science issues. Thus, the delocalization effects that determine the molecular aromaticity share the same causal reasons with those driving the optical and electrical properties of polymeric conducting polyenes [4,5] and the special properties of nanoscale graphenes. [6]

---

<sup>a</sup> University of Bucharest, Faculty of Chemistry, Inorganic Chemistry Department, Dumbrava Rosie 23, Bucharest 020462, Romania. [marilena.cimpoesu@g.unibuc.ro](mailto:marilena.cimpoesu@g.unibuc.ro)

<sup>b</sup> Institute of Physical Chemistry, Splaiul Independentei 202, Bucharest 060021, Romania. [cfanica@yahoo.com](mailto:cfanica@yahoo.com)

As offers-and-demands balance, there is a large variety of models devoted to the aromaticity, in answer to the general appeal of this topic, along the time-line of modern and contemporary chemistry. The models address, at various levels, electron structure parameters, going from semi-empirical conventions, such as the TREPE indexing (Topological Resonance Energy Per Electron) [7] to criteria worked by *ab initio* procedures, as the NICS case (Nucleus Independent Chemical Shifts) [8], keeping also correlations with instrumental checking *via* NMR shifts. [9] The above mentioned methods are usable also in the generalized purposes, for assessing the aromaticity in non-organic systems, going then beyond the classical early outline of the concept (namely, the Kekule-Erlenmeyer identification with the presence of benzene rings, [10] and the pioneering Hückel rules [11] of  $(4n+2)\pi$  electron count in planar conjugated hydrocarbons).

Once the structural patterns of the extremely large variety of cluster systems started to be rationalized with the help of electron-count Wade-Mingos rules, [12] it became clear that aromaticity has rich manifestations in the realm inorganic and organometallic rings and clusters.[13,14] From its initial limitation to planar molecules, the aromaticity was generalized to three-dimensional and spherical patterns. [15]

In the key of such paradigms, the chemistry offers large open and uncharted areas, tempting audacious prospectors with promising new treasures. To answer this challenge, a good general culture in intricacies of cluster chemistry and structural methods is demanded. Fulfilling such commandments, a fine collection of correlations between cluster stereochemistry and electron counting concepts is offered by the works of Professor Ioan Silaghi-Dumitrescu. [16] At the same time, several aspects marked at the study of clusters with distorted polyhedral frames [17] can be presented as inquires open to the anti-aromaticity case studies. The puzzling case of electron  $\text{Ge}_{12}^{2-}$  cluster [18] showing high symmetry combined with antiaromatic-type NICS indices, i.e. putting in sheer contradiction the criteria of bond length distribution vs. ring-current determinations, proves the challenge of the running paradigms and the value of the heritage offered by professor's Silaghi-Dumitrescu works, his topics pointing the way to new exploratory paths. Honoring such achievements, we will present selected parts from our investigations on several systems proposed as prototypic examples, illustrating the variety of landscapes in the realm of aromaticity concepts.

## RESULTS AND DISCUSSION

### ***1. Revisiting the basic organic prototypes: aromaticity in $\text{C}_6\text{H}_6$ and the antiaromaticity of $\text{C}_4\text{H}_4$***

We will set our starting point with the most celebrated representatives of the aromaticity-antiaromaticity dyad, namely the benzene and cyclobutadiene, respectively. In complex polyaromatic hydrocarbons,[3] the existence of aromatic

type behaviour and properties is usually associated with the presence of blocks made of conjugated six-membered rings. For anti-aromaticity the situation is different, since there are no notorious cases of globally antiaromatic molecules assigned to the presence of smaller antiaromatic building blocks. The anti-aromatic behaviour is manifested in different ways, most generally characterized by the presence of a distortion (C=C and C-C bond length alternation and the eventual non-planarity of the rings). Conversely, the aromaticity can be generally presented as resistance to distortion, the system adopting the most symmetrical molecular geometry, with respect of the given topology. The anti-aromatic bond length distortion can be considered a pseudo-Jahn Teller effect [19] and the aromaticity itself can be outlined as balance of factors related to the  $\pi$ -distortivity effects.[2a] We revisited [20] the antiaromaticity of these two systems combining state of the art CASSCF (Complete Active Space Self Consistent Field) calculations and the vibronic modelling, a complex approach taking into account the coupling between vibration and electronic factors. [21] The methodological procedures are not trivial, since, even though the computer codes for structural chemistry have become increasingly accessible, powerful and user-friendly, it is not a simple task to recover from the massive black box of an *ab initio* calculation the pieces needed to recover a picture in line with the chemical intuition perspectives. For instance, the general knowledge takes the  $\pi$  problem at benzene as a frontier MO picture, while using Hartree-Fock (HF) as starting procedure, and 6-311+G\* basis set we must retrieve the set of six  $\pi$ -type molecular orbitals (belonging to the  $a_{1u}$ ,  $e_{1g}$ ,  $e_{2u}$ ,  $b_{2g}$ , representations of the  $D_{6h}$  point group) from the positions 12, 15, 16, 22, 23, 48, respectively (the HOMO-LUMO couple being located at the 21-22 sequence).

Therefore, to set-up a CASSCF procedure one must construct the active space with carefully selected molecular orbitals, the use of chemical intuition being a key step in the art of this kind of multi-configuration calculations. The CASSCF(6,6) calculation (where the numbers in brackets specify the use of 6 electrons in 6 orbitals) produces 175 spin singlet states. We identified the series of 1,3,9,10, 22 levels as being relevant for interpreting the results in terms resonance concepts. Thus, the mentioned series of states can be presented as superposition of the celebrated resonance structures of Kekule and Dewar type. As suggested on Fig.1b chart also, the first two states (the  $^1A_{1g}$  groundstate and the  $^1B_{2u}$  excited one) can be presented, respectively, as the *in-phase* (sum) and *out-of-phase* (difference) of Kekule-type resonance structures. The upper three levels are combination of Dewar-type resonances (a degenerate couple  $^1E_{2g}$  and a totally symmetric combination with equal weights of all three components). We have selected 5 relevant states out of the many CASSCF levels, to span their making from 5 resonance structures, the identification of the adequation to this phenomenology being checked by rather complicate succession of steps.

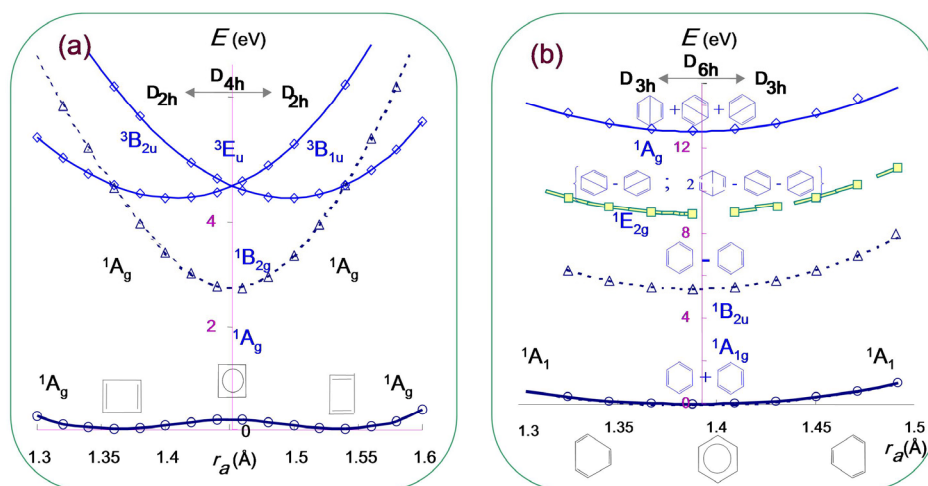


**Figure 1.** Energy profiles, as function of bond alternating distortion, for selected ground and excited states of: a) cyclobutadiene b) benzene. One observes the pseudo Jahn-Teller effect (double well potential energy of the ground state) that correspond to the anti-aromaticity. The aromaticity is interpreted as resistance against distortion trend (parabola profile). The states were selected from the set of CASSCF calculations to correspond to the interpretation in terms of resonance structures.

The resonance ideas are sometimes presented in as puzzling, suggesting the physical non-reality of separate resonance structures. In fact, the resonance structures are not so imaginary things, neither bogus nor counterfeit. These are the quite concretely writable wave-functions, serving to obtain a given set of states, by their linear combination. In both  $C_6H_6$  and  $C_4H_4$  cases, the ground state can be taken, at the point of high symmetry, as the  $\Psi_{\text{sym}} \propto (K_1 + K_2)$  superposition of the two Kekule resonances, while the first excited one is the  $\Psi_{\text{asym}} \propto (K_1 - K_2)$  combination. The aromaticity is then characterized by keeping the high molecular symmetry and the correspondingly symmetrical superposition of resonance components. The antiaromaticity can be considered as the trend toward a distorted state, by adopting a pattern adequate for a given single resonance component (i.e. having alternating bonds according to the single vs. double character), i.e. either  $K_1$  or  $K_2$ , as shown in different extremes of the panel a of Figure 1.

Conversely, the individual resonance structures can be presented as a mixing between ground and excited states, as these were defined in the high symmetry point, e.g.  $K_1 \propto (\Psi_{\text{sym}} + \Psi_{\text{asym}})$  or  $K_2 \propto (\Psi_{\text{sym}} - \Psi_{\text{asym}})$ . Then, the antiaromaticity can be formulated as this kind of interstate coupling, promoted by a distortion coordinate. It is, therefore, a case of vibronic coupling or, in other words, a pseudo Jahn-Teller effect. The pseudo Jahn-Teller effect,[19]

i.e. the spontaneous distortion of a symmetrical system with non-degenerate groundstate, is a balance of two opposite terms: a so-called vibronic part, that cumulates all the effects due to the mixing between ground and excited states, and a non-vibronic element that contains all the remaining effects.

The vibronic modeling, comprising terms that account for the dynamic factors, has more general virtues even in cases when there is no distortion of Jahn-Teller or pseudo Jahn-Teller type. The force constant for any given nuclear coordinate can be put as a sum of non-vibronic and vibronic terms,  $k=k_0+k_v$ . The non-vibronic term can be intuitively interpreted as a sort of mechanical resistance of the molecular skeleton against the given distortion. The pseudo Jahn-Teller distortion becomes visible when the vibronic term ( $k_v<0$ , that gives negative contribution to the force constant with respect of a nuclear distortion coordinate) dominates the non-vibronic one ( $k_0 > 0$ , a positive contribution). In the frame of vibronic modeling the aromaticity and antiaromaticity can be then presented as two cases of a common mechanism, based on the mixing of two states  $\Psi_{\text{sym}} \propto (K_1+K_2)$  and  $\Psi_{\text{asym}} \propto (K_1-K_2)$  which yields a  $k > 0$  parameter for aromaticity and  $k < 0$  for antiaromaticity. Our analyses showed that the  $\pi$  subsystem contributes in both aromatic and antiaromatic cases to the vibronic component  $k_v < 0$ , while the nonvibronic one can be mostly assigned as due to the  $\sigma$  skeleton. Or, in other words, if only the  $\pi$  system existed, even the benzene would have been distorted. The  $\sigma$  skeleton is stronger in the case of benzene, because of in-plane hybrids matching perfectly the  $120^\circ$  bond angles. Then,  $k_0$  predominates, leading to the conservation of the symmetric frame. The  $90^\circ$  bond angles in cyclobutadiene can be obtained only with pure  $p$  orbitals, loosing then the cohesive supplement from the  $s$  shell. Having a smaller positive  $k_0$ , determined by the weaker skeleton, the cyclobutadiene becomes the subject of the pseudo Jahn-Teller distortion. The energy profile of the ground state along the bond-alternating distortion shows two minima, corresponding to molecular frame distorted in rectangular way, the symmetrical square configuration being metastable, as transition point between these rectangular optimal geometries. Conversely, the energy profile for the benzene ground state is a parabola with minimum in the hexagonal symmetry.

Since the CASSCF, as electron structure calculation method, implies certain intricacies, we will attempt to commute now in presenting the aromaticity issue in more affordable frames, such as the Density Functional Theory (DFT).[22] In this view, *a posteriori*, to a B3LYP/6-311G\* calculation for benzene, which is a straightforward task, we employed several steps worked with the help of Natural Bond Orbital (NBO) method.[23] Namely, localized orbital functions were obtained by corresponding input specification of the desired atom pairs. Thus, in one case we specified the three double bonds located between C1-C2, C3-C4 and C5-C6 couples, in order to mimic one Kekule structure (See panel a in Figure 2).

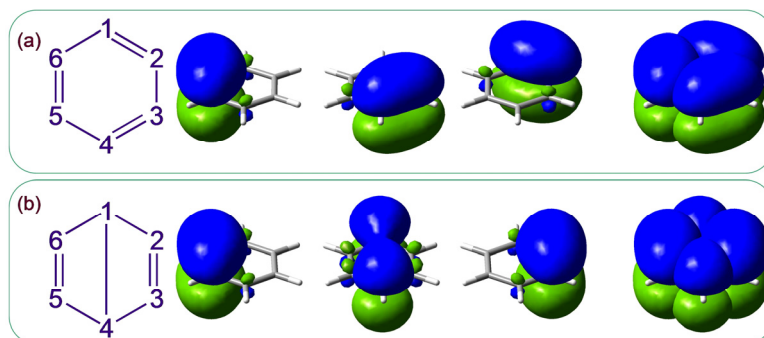


**Figure 2.** Computational experiments simulating the (a) Kekule and (b) Dewar resonance structures with the help of localized bond orbitals and enforced occupation of each state with a pair of electrons. In the right side, the superpositions of three individual orbitals from each set are presented.

Aiming for a Dewar structure, we succeeded in producing a distant C1-C4 weak bond, aside the regular C2-C3 and C5-C6 double bonds (See Figure 2b). This result is a non-standard approach, but at the same time can be worked in user-friendly manner, since the NBO code[24] can be easily controlled by specifying the desired connectivities and formal bond orders. If one imposes the double occupation of these localized bond orbitals, the total density breaks the hexagonal symmetry, showing the Kekule or Dewar  $\pi$  alternation patterns. One must point that this approach is different from the the so-called Natural Resonance Theory (NRT) [25] also related to the NBO frame. Another computational experiment consisted in taking these broken symmetry total densities and doing a non-iterative DFT calculation with the imposed frozen functions. The resulted energies are higher than those from regular DFT calculation, the gap measuring the stabilization gained by the molecular orbital delocalization. If one s the energy gap by 6, one obtains an equivalent of topological resonance energy per electron (TREPE). While the standard TREPE [7] is a semiempirical procedure based on Hückel-type approach, our computation experiment offers quantities resulted from state of the art DFT techniques. The corresponding amounts (per electron) are 0.10 a.u. (60.8 kcal) for the Kekule state and 0.42 a.u. (265.3 kcal) for the Dewar case. The above revisiting of the very classical prototypic systems of the aromaticity paradigm gave us the opportunity to present and assess methodological issues that can be applied on other examples of general aromaticity, as we will proceed in the following.

## ***II. The spherical aromaticity in inorganic systems. The icosahedral borane***

The  $B_nH_n^{2-}$  dianions were assigned as aromatic[26] with the help of NICS indices,[8] having a new manifestation, i.e. the spherical aromaticity. This happens because the orbitals of the clusters having the atoms averagely distributed on the surface of a sphere, start to approximate, progressively with the increase of nuclearity, certain regularities similar to a giant atom virtually placed in the center of the cluster and carrying in its shells the valence (bonding and nonbonding) electrons of the constituents. The sign of the orbital components resemble the pattern known for atomic orbitals, or more precisely, the Spherical Harmonics angular functions. In Figure 3 a comparison of classical planar aromaticity with the 3D generalization is suggested. The aromaticity in rings is related to the circular symmetry, whose representations are driven by the  $\exp(\pm iM\phi)$  functions, or equivalently, by the  $\{\cos(M\phi), \sin(M\phi)\}$  couples. These form doubly degenerate shells, except the  $M=0$  element, which is the trivial total symmetrical representation. Filling progressively the  $M=0, 1, 2, \text{ etc}$  sub-shells drawn in the panel (a) of Figure 3, one obtains the 2, 6, 10, ... electron count, spanning the  $4n+2$  Hückel rule. In clusters, we go to higher spherical patterns. Here, the irreducible representations are Spherical Harmonics with  $L=0, 1, 2, \dots$  parameters, that are similar to the atomic shells, i.e. having a  $2L+1$  multiplicity and  $L$  nodal planes in each subset. The lobes of the MOs constructing a pseudo-spherical cluster are "painted" in "colors" borrowed from the pattern of the Spherical Harmonics depicted in the panel (b) of Figure 3. More precisely, the LCAO components of an AO located at a given position on the sphere are proportional in sign and magnitude with the Spherical Harmonics at that coordinate. Then, the MOs are grouped in quasi-degenerate sets spanning the  $2L+1$  multiplicities of an appropriate  $L$  number. Then, progressively filling such sub-shells one obtains a 2, 8, 18, series, i.e. a  $2(L+1)^2$  count. Such a regularity is called the Hirsch rule. [27] Since in many cases the effective symmetry is not so high, to completely match the spherical approximation, and also because the full complexity of electron structure is realized with the help of supplementary functions taken as derivatives of Spherical Harmonics, there are alternate regularities, such as Wade's electron count, which specifies the need of  $2n+2$  polyhedral skeleton electron pairs [28] to achieve a good stability and therefore to claim the aromaticity case. Counting the valence electrons in the  $B_{12}H_{12}^{2-}$  as follows,  $12 \times 5$  from boron atoms, 12 from hydrogens and 2 from dianion charge, one obtains a total of 50 electrons, apparently favorable to the Hirsch rule (with  $L=4$ ). Counting the skeletal electron pairs (i.e. ignoring the  $12 \times 2$  electrons comprised in the outer B-H bonds) one obtains a 26 count that satisfies Wade's rule for the electron pairs devoted to the cluster itself.

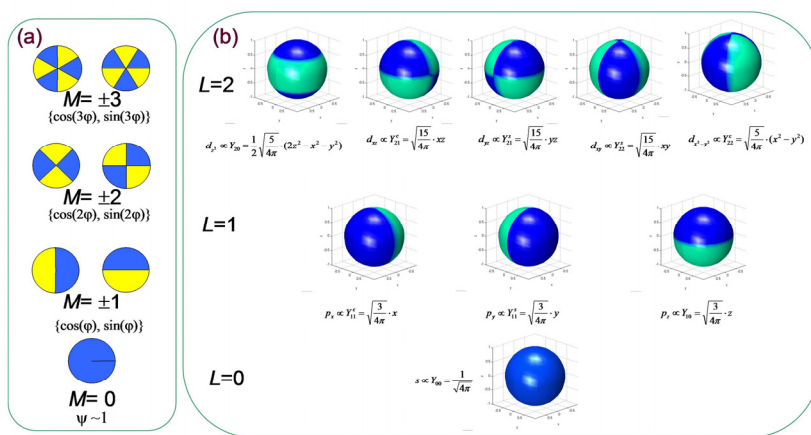


**Figure 3.** Symmetry regularities determining the aromaticity in (a) rings and (b) clusters, according to the patterns of cyclical and spherical symmetry, respectively. The different colors mark the different signs of the functions and nodal planes around a cycle and on the surface of a sphere.

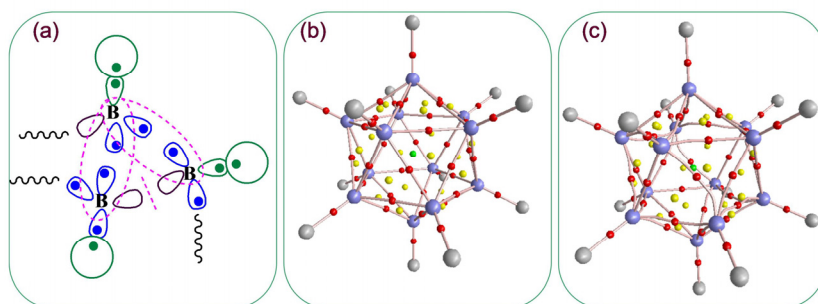


**Figure 4.** The bonding regime in boranes. a) the scheme of local electron deficiency, each B atom contributing with two electrons for the cluster; the possibility to assign formal localized bonds on and electron void areas is suggested. (b) The  $B_{12}H_{12}^{2-}$  dianion with its critical points and bond paths. (c) The bond paths in the neutral  $B_{12}H_{12}$  appear curved and distorted, as expression of the fact that the electron count of the neutral molecule is incompatible with a stable closed shell icosahedral configuration.

Besides, looking at point group symmetry reasons, one observes that the dianion realizes the completion of a four-degenerate HOMO level. This is why the dianion status is required, because otherwise the non-closed degenerate shell would lead to pseudo Jahn-Teller distortions. From this point of view, the neutral  $B_{12}H_{12}$  could be called anti-aromatic. However, the things are a bit more complicated.



Another view on the aromaticity of boranes is the electron deficient nature of the boron. This implies a large delocalization, in order to spread the electron density over all the interatomic contacts. Employing the analysis of density distribution with the help of Bader's theory of Atoms in Molecules (AIM) [29, 30] one obtains the so called (3,-1) critical points, certifying the formation of a bond for each B-H unit and also for all the 30 B-B edges of the icosahedron, both in case of the dianion  $B_{12}H_{12}^{2-}$  and for the neutral  $B_{12}H_{12}$ . The number of established bonds is larger than the available electron pairs (13 for dianion, 12 for the neutral molecule). It is interesting to compare the bond paths of the two related systems (depicted in Figures 4b and 4c). The bond paths are gradient lines joining points of maximal density located at nuclei, passing via the (3,-1) bond points. Regular bond paths are almost linear, while in certain cases these appear curved, as is visible for the neutral  $B_{12}H_{12}$ . Because of incomplete degenerate HOMO shell, the neutral  $B_{12}H_{12}$  is unstable in the icosahedral symmetry, but we will discard for the moment the question of optimal geometry and the comparison of distortion isomers. In turn, the bond path bending resulted by taking the enforced icosahedral symmetry for  $B_{12}H_{12}$  can be interpreted as a sign of the inner trends for distortion.

In the following we will try to transcribe the electron deficient boranes in terms of resonance structures. Because the number of electron pairs is larger than the number of interatomic bonds, the groundstate must be conceived as a superposition of many configurations. Each boron atom participates with two electrons to the cluster delocalization, while one electron per boron should be reserved for firm bonds with the outer hydrogen atoms. Each boron has 5 immediate neighbors, but is able to share Lewis-type electron pairs only with two of them. Each B atom has formally an empty valence orbital (See the panel a of Figure 3).

Therefore, if draw a line for an electron pair shared by a B-B couple, each boron vertex of the  $B_{12}$  polyhedron has two emerging lines. The resonance structures can be then formulated as lines running over a total of 12 edges in the case of  $B_{12}H_{12}$  and over 13 edges in the case of  $B_{12}H_{12}^{2-}$  dianion. It is particularly more convenient to discuss the resonance structures of the neutral molecule. We will not detail now their complete count, which is a matter of specialized graph theory. We will confine ourselves in noticing that, marking by ticker lines the bonds, these can be grouped in a number of closed walks, ranging from 1 to 4 independent circuits (See Figures 5-7).

These circuits do not cross each-other and comprise, in ensemble, all the vertices of the icosahedron. In the case of the dianion  $B_{12}H_{12}^{2-}$  one supplementary line can be drawn at any of the 18 remaining empty B-B lines (out of the 30 B-B edges) to which no previous line was assigned (12 edges being occupied by the mentioned bond lines). Each possibility to design such walks can be considered as a resonance structure. The superposition of such resonance structures resolves the problem of electron

deficiency and consequently offers a suggestion for the aromaticity of these systems, if accepting that aromaticity can be defined as the need for resonance superposition, in order to describe a stable structure. In this perspective, even the neutral  $B_{12}H_{12}$  can be presented as aromatic while  $B_{12}H_{12}^{2-}$  is the most aromatic, since it has more resonance structures, multiplied by a factor of 18 as compared to the  $B_{12}H_{12}$  count as seen above.

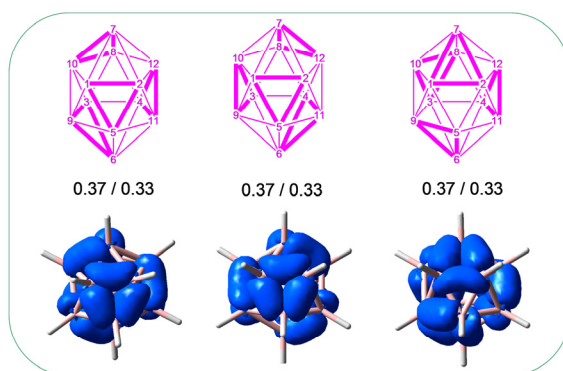


**Figure 5.** Selected equivalent resonance structures for  $B_{12}H_{12}$ , spanning 4 islands of 3-membered circuits, marked with bold lines in the graphs depicted in the upper part. The lower part contains the simulation of this resonance structure with the help of superposed correspondingly prepared and occupied localized bond orbitals. The numbers written in couples on the middle line are designed as a measure of resonance effect: the first number of each couple is estimated for dianion and the second for the neutral molecule. Each values represents the DFT energy gap (in a.u.) of between the localized resonance structure and the delocalized state, divided by 24, the number of cluster electrons, in order to have a resemblance with TREPE indices.

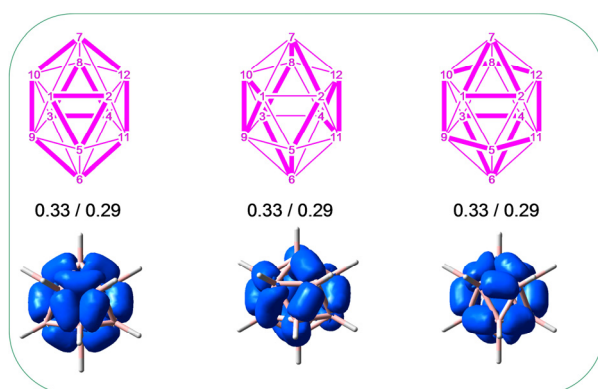


**Figure 6.** Selected equivalent resonance structures spanning 3 islands with 3,6,3 members. The interpretation is similar to the precedent figure.

The neutral system can be presented, at this stage, as intermediately aromatic, since, even letting it to relax at a lower symmetry the presence of resonance superposition will still be required to resolve its intrinsic electron deficiency. The complete picture will not be developed now. We will proceed, in turn, to an interesting computational experiment, mimicking the above mentioned types of resonance structures with the help of localized natural bond orbitals, using the same procedures as explained in the above section for benzene. This simulation of the resonance structures is a rather inedited deal, as well as, to the best of our knowledge, the whole explained picture of resonating bonds in boranes. The procedure offers also certain indices similar to the traditional TREPE, as explained above in the benzene case. We recall that, to be distinguished from TREPE, which are based on empirical methods, our approach is based on energy amounts primarily obtained at DFT level. Thus, the energy gap between the DFT energies of delocalized molecule and enforcedly localized resonance structure, divided by the number of electrons in the cluster, i.e. 24, stands for the values printed along with the resonance structures from figures 5-7. The values are presented in couples, the first one devoted to the dianion, the second to the neutral molecules. The resonance structures are, in fact drawn for the neutral molecule, the dianion presenting a supplementary number of resonances, due to the added electron pair. In our calculations the dianion was taken by a resonance structure obtained adding a lone pair, conventionally, on the first atom, B1. The definition as lone pair is convenient because in this way it appears delocalized towards the remaining boron neighbours and offers in this way a sort of simulated averaging over the three resonance structures obtainable by separate localization procedures. One observes that the defined indices show larger magnitudes for the dianion, as a measure of its larger aromaticity. At the same time, even though the resonance patterns differ very much in topological respects, their indices are comparable, suggesting that the resonance in borane may use such various patterns on almost equal footing. The pictures 5 and 6 offer, altogether with the formal resonance structures, the realistic electron density superposition realized with the localization approach. The figure 7 is confined to drawing only the formal graphs of several other selected resonances, altogether with their corresponding indices. In panel 7a is illustrated another topology with 3 rings of bond circuits, in 7b patterns with two 6-membered circuits, in 7c selected shapes with two unequal circuits (3 and 9 membered) and in 7d the case of single 12 member circuits. The classification of the resonance structures in the above suggested style is a challenging matter in itself, as graph theory issue, committing our interests in further developments in this sense.

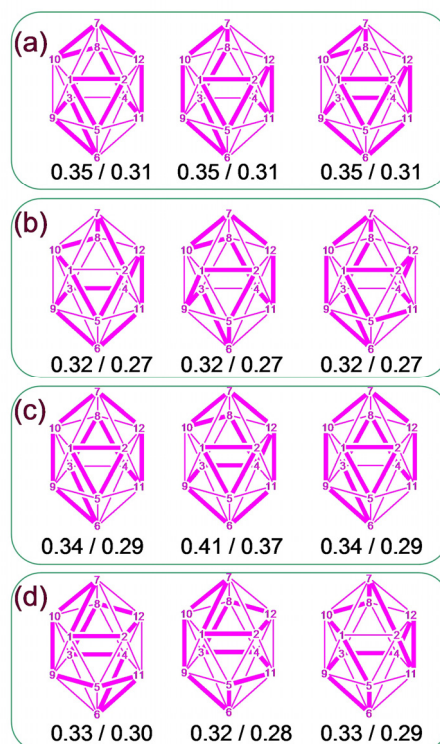


**Figure 7.** Selected equivalent resonance structures of  $B_{12}H_{12}$ , belonging different topological patterns : a) 3 circuits with 3,6,3 members; b) two circuits with 6,6 members; c) two circuits with 3,9 members; d) a single circuit with 12 members. The value couples below each graph are resonance indices for dianion and neutral cases, respectively.

### ***III. The aromaticity in coordination systems. The diketonate ligands***

The diketonate anions can be proposed as subject for inquires on aromaticity, since their structure with delocalized negative charge imply the use of resonance structures. We will address this issue in both the free anion and also coordination complexes with diketonates as ligand, using in this purpose the the so-called Natural Resonance Theory [25] which is a part of the NBO methods and computer codes.[23] The procedure is a bit different from our previously exposed methodology with localized orbitals and is distinct also from the genuine frame that imposed the concept of resonance, namely the Valence Bond theory (VB). [31] The NRT is not a multiconfigurational method. It offers a sort of surrogate for the effect of

superposed resonance structures, fitting the total density from a regular DFT calculation (i.e. with delocalized MOs) in terms of contributions from occupation schemes with imposed localizations. This procedure offers a convenient user-friendly access to the resonance concepts.

We will take as study case a coordination system from our own synthetic results,[32]  $[\text{Ni}(\text{tmen})(\text{NO}_2)(\text{dbm})]$ , where *tmen* is tetra-methylene-diamine and *dbm* is dibenzoyl-methanate, i.e. the diketonate taken in our focus. In Figure 8 we comparatively show the weights of main resonance structures for the free ligand and the coordinated one. The presented amounts do not complete a 100% total, since there are several other discarded small terms, assignable to hyperconjugation effects. The free ligand is less aromatic, since the contribution of the keto-enolate forms are smaller, being in competition with a carbanionic resonance. In the coordinated mode, the two keto-enolate resonance structures become the dominating contributors. In the presented case, the two twin diketonate resonances have slightly differing weights because of the asymmetry induced by the mixed ligand environment. The chelate can be interpreted as aromatic, since it can be presented as superposition of two equivalent resonance structures.

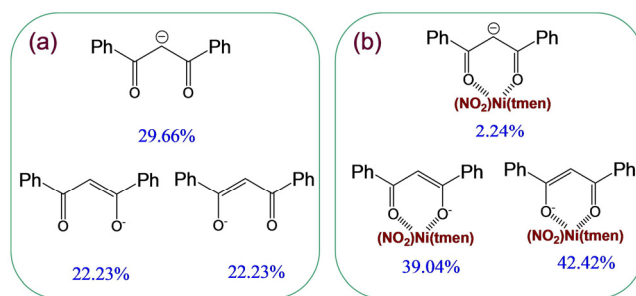


**Figure 8.** The resonance weights computed with the NRT (post DFT) method for the: (a) free and (b) coordinated, dibenzoyl-methanate ligand.

#### IV. Surface aromaticity in organometallic clusters

We will propose as example for this entry a system belonging to our previous work, a carbalane cluster with  $\{\text{Al}_8\text{C}_6\}$  cubo-octahedral pattern.[33] Not only the theoretical analysis, but also the chemical tests suggested this system as aromatic, since the cluster core resisted well at several reactions that affected only its terminal groups, in a manner resembling the stability of benzene core against substitutions and additions. This cluster is electron deficient (like boranes), since the analysis of critical points of density identified implying the superposition of resonance structures, as suggested by panel more bonds than the available electron pairs, as seen in Figure 9a, the situation 9b.

There are  $4^6 = 4096$  resonance structures, figure 9b presenting only a selected portion. Without entering the details, we point that there exist two different types of Al-C bonds, differing by certain overlap factors, one marked with full line, the others with dashed line. From each C site emerges one tick line and two dashed ones.

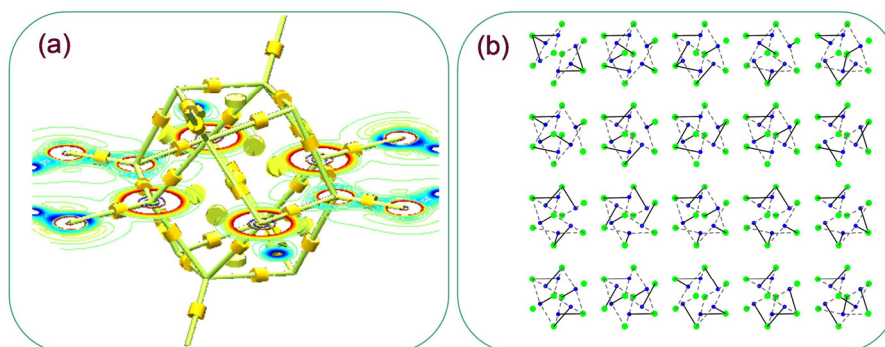


**Figure 9.** Synopsis of the delocalization and resonance effects in the carbalane with  $\{Al_8C_6\}$  core, as images of surface aromaticity effects. The skeleton drawn in (a) corresponds to computed bond paths, with bond critical points marked with ticker cylinders. The C atoms are penta-conexe (with 4 bonds inside the cluster and one outer one, while the aluminum are represented as triconexe). The Laplacian of electron density is represented in a molecular section. In (b) one shows a selected part of the resonance structures with linkages between the the  $Al_8$  and  $C_6$  subsystems.

The resonance structures at one  $\{Al_4C\}$  face of the cluster are obtained rotating the set of three bonds around the square frame, letting one Al site non-bonded. The rule for obtaining the resonance structures can be presented as decrypting the monomials resulted after expanding the following product:

$$\begin{aligned} & (y_1x_2y_3 + x_1y_2y_4 + y_1y_3x_4 + y_2x_3y_4) \cdot (y_5x_6y_7 + x_5y_6y_8 + y_5y_7x_8 + y_6x_7y_8) \cdot \\ & (x_1y_2y_5 + y_1x_2y_6 + y_1x_5y_6 + y_2y_5x_6) \cdot (x_2y_3y_6 + y_2x_3y_7 + y_2x_6y_7 + y_3y_6x_7) \cdot \\ & (x_3y_4y_7 + y_3x_4y_8 + y_3x_7y_8 + y_4y_7x_8) \cdot (x_1y_4y_5 + y_1x_4y_8 + y_1x_5y_8 + y_4y_5x_8) . \end{aligned}$$

The  $x_i$  (with  $i = 1$  to  $8$ ) stand for the aluminum the Al-C bonds conventionally marked by tick line, while the  $x_j$  represent the dashed ones. The subscript indices mark the Al atom touched by the bonds of the presented types.

### V. An inedited case of supramolecular antiaromaticity

We present now a system with radicalic character that can be exploited as an unprecedented case of antiaromatic-type distortion in a supramolecular ordered network. The compound was synthesized[34] and explored by us for sake of magneto-structural correlations, the antiaromatic features remaining yet incompletely explored, presenting here an excerpt of the ongoing detailed analysis. The system is an octa-coordinated yttrium complex  $K[Y(QT)_4]$  with QT (Quinoline-Tempo) a diketonate chelatic ligand that has also a radical tail. The interaction between the NO radical groups of the ligand tails and the lattice potassium ions determines a supramolecular ordering with nodes made of  $K^+$  ions surrounded by four radicals. The set of four interacting radicals resembles the configurational problem from the cyclobutadiene prototype (4 electrons in 4 orbitals). Even though here there is not the case of similar genuine  $\pi$  system, the same factors that determine the rectangular shape of  $C_4H_4$ , are imposing the distortion in the actual  $\{K(QT)_4\}$  moieties of our system.

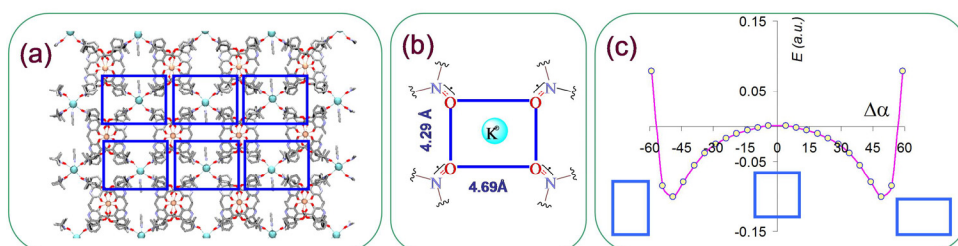


**Figure 10.** (a) The antiaromatic-type rectangular distortions in the supramolecular assemblies of the  $K[Y(QT)_4]$  complex with radicalic ligands. (b) The scheme of the  $\{K(QT)_4\}$  node with four-radical character and rectangular pattern. (c) A simplified simulation of the preference for distortion in the idealized model model  $[K(ONH_2)_4]^+$  of the four radical complex node. The  $\Delta\alpha$  coordinate measures the deviation of one O-K-O angle from the  $90^\circ$  perfect square value. Namely, at the perfect square geometry  $\Delta\alpha=0$ , the energy profile shows a metastable transition point, the system spontaneously breaking its symmetry toward the minima corresponding to antiaromatic pattern.

The rectangular pattern of the whole supramolecular ordering is shown in Figure 10a, with the scheme of rectangular  $\{K(QT)_4\}$  nodes in 10b. In 11c we present a simulation of the preference for distortion, taken on a simplified model  $[K(ONH_2)_4]^+$  with B3LYP/6-311G\* DFT potential energy surface procedures. The double well potential proves the trend for the antiaromatic type of distortion in the four radical system, an effect which is cooperatively transmitted to the whole supramolecular network.

The system is interesting also from magneto-structural point of view, being a challenging detective story. Namely, the attempts to fit the experimental magnetic susceptibility with standard procedures lead systematically to results incompatible with the experimentally observed rectangular topology. The cause was a sort of accidental local minimum comprised in the standard phenomenological modeling. A clear cut of the question was done with the help of *ab initio* calculations, that helped us in choosing the right parametric balance, the situation being illustrative for the role of theoretical approaches, as valuable complements to experiments.

## CONCLUSIONS

We presented a broad perspective on the aromaticity paradigm, analyzing prototypic molecules such as benzene and icosahedral boranes, as examples for organic and inorganic cases, and systems from our own results, to illustrate the coordination, [32] organometallic [33] and supramolecular [34] varieties. The aromaticity is a very generalizing and fruitful keyword, that catalyzes interdisciplinary results, establishing natural bonds between the experimental and theoretical sides. It is important to safeguard these links and the role of intuition, since with the advent of modern electron structure methods and codes, the thesaurus of heuristic ideas like hybridization, hypervalence, aromaticity, started to loose terrain in the front of accurate *ab initio* reproduction of structural parameters. The brute-force computational approach does not need, apparently, the *a priori* guidelines of these heuristic concepts originating from the experimental chemistry, but a real understanding is realized when we can find a simple meaning behind the output bulk information. It is a challenge to rebuild *a posteriori*, from the bare output of the electronic structure methods, the information matching the major keywords with *aprioric* virtues. The revisiting of the basic concepts is a steady temptation and a challenging task, with a rewarding outcome. In spite of its longstanding history, the aromaticity is still an active and appealing concept, that triggers theoretical debates and marks the way to new lands of experimental chemistry.

## EXPERIMENTAL SECTION

The synthetic and structural details of the compounds belonging to our synthetic works were presented elsewhere. [33, 34]. The calculations were performed using the Gaussian 03,[35] Gamess [36] and NBO [24] software packages.

## ACKNOWLEDGMENTS

Parts of this work were supported by the CNCSIS-UEFISCSU grant "Idei" 174/2007.



## REFERENCES

1. (a) L. Salem, "The Molecular Orbital Theory of Conjugated Systems", Benjamin, New York, **1966**. (b) V. I. Minkin, M. N. Glukhovtsev, B. Y. Simkin, "Aromaticity and Antiaromaticity", Wiley, New York, **1994**.
2. (a) S. Shaik, A. Shurki, D. Danovich, P. C. Hiberty, *Chem. Rev.*, **2001**, *101*, 1501. (b) P. v. R. Schleyer, H. Jiao, *Pure Appl. Chem.*, **1996**, *68*, 209.
3. (a) E. Clar, "Polycyclic Hydrocarbons", Academic Press, London, **1964**. (b) T. M. Krygowski, M. K. Cyranski, Z. Czarnocki, G. Häfeli, Alan R. Katritzky, *Tetrahedron*, **2000**, *56*, 1783.
4. (a) Z. Shuai, J. L. Bredas, *Physical Review*, **2000**, *B 62*, 15452. (b) W. Barford, R. J. Bursill, *Physical Review*, **2006**, *B 73*, 045106.
5. Y. Geerts, G. Klärner, K. Müllen, "In Electronic Materials: The Oligomer Approach", K. Müllen, G. Wagner, Eds.; Wiley-VCH:Weinheim, Germany, **1998**.
6. J.-N. Fuchs, P. Lederer, *Physical Review Letters*, **2007**, *98*, 016803. (b) B. Trauzettel, D. V. Bulaev, D. Loss, G. Burkard, *Nature Physics*, **2007**, *3*, 192.
7. (a) I. Gutman, M. Milun, N. Trinajstić, *J. Am. Chem. Soc.*, **1977**, *99*, 1692. (b) J. Aihara, *J. Am. Chem. Soc.*, **1976**, *98*, 2750; **1977**, *99*, 2048. (c) M. S. J. Dewar, C. de Llano, *J. Am. Chem. Soc.*, **1969**, *91*, 789. (d) A. Graovac, I. Gutman, M. Randić, N. Trinajstić, *J. Am. Chem. Soc.*, **1973**, *95*, 6267. (e) A. R. Katritzky, K. Jug, D. C. Oniciu, *Chem. Rev.*, **2001**, *101*, 1421.
8. P. v. R. Schleyer, C. Maerker, A. Dransfeld, H. Jiao, N. J. R. v. E. Hommes, *J. Am. Chem. Soc.*, **1996**, *118*, 6317.
9. (a) P. v. R. Schleyer, H. Jiao, *Pure Appl. Chem.* **1996**, *68*, 209. (b) T. M. Krygowski, M. K. Cyrański, Z. Czarnocki, G. Häfeli, A. R. Katritzky, *Tetrahedron*, **2000**, *56*, 1783.
10. (a) A. Kekulé, *Bull. Soc. Chim. Fr.*, **1865**, *3*, 98. (b) E. Erlenmeyer, *Liebigs Ann. Chem.*, **1866**, *137*, 327.
11. E. Hückel, *Z. Physik*, **1931**, *70*, 204; *Z. Physik*, **1931**, *72*, 310; *Z. Physik*, **1932**, *76*, 628.
12. (a) K. Wade, *Chem. Commun.*, **1971**, 792. (b) D. M. P. Mingos, *Acc. Chem. Res.*, **1984**, *17*, 311.
13. (a) R. B. King, *Chem. Rev.*, **2001**, *101*, 1119, and references therein. (b) R.B. King, *Inorg. Chim. Acta*, **2003**, *350*, 126. (c) H. Tanaka, S. Neukermans, E. Janssens, R. E. Silverans, P. Lievens, *J. Am. Chem. Soc.*, **2003**, *125*, 2862.
14. (a) A. I. Boldyrev, J. Simons, *J. Am. Chem. Soc.*, **1998**, *120*, 7967. (b) X. Li, A. E. Kuznetsov, H. F. Zhang, A. I. Boldyrev, L.-S. Wang, *Science*, **2001**, *291*, 859. (c) A. Hirsch, Z. Chen, H. Jiao, *Angew. Chem.*, **2001**, *113*, 2916; *Angew. Chem., Int. Ed.*, **2001**, *40*, 2834.

- 
15. (a) A. Hirsch, Z. Chen, H. Jiao, *Angew. Chem., Int. Ed.*, **2001**, *40*, 2834. (b) M. Bühl, A. Hirsch, *Chem. Rev.*, **2001**, *101*, 1153.
16. (a) R. B. King, I. Silaghi-Dumitrescu, *Inorg. Chem.*, **2003**, *42*, 6701. (b) R. B. King, I. Silaghi-Dumitrescu, A. Lupan, *Inorg. Chem.*, **2005**, *44*, 3579. (c) R. B. King, I. Silaghi-Dumitrescu, A. Lupan, *Inorg. Chem.*, **2005**, *44*, 7819. (d) R. B. King, I. Silaghi-Dumitrescu, M. M. Uță, *Inorg. Chem.*, **2006**, *45*, 4974.
17. (a) R. B. King, I. Silaghi-Dumitrescu, A. Kun, *Inorg. Chem.*, **2001**, *40*, 2450. (b) R. B. King, I. Silaghi-Dumitrescu, M. M. Uță, *J. Chem. Theory Comput.*, **2008**, *4*, 209.
18. (a) R. B. King, I. Silaghi-Dumitrescu, M. M. Uță, *Dalton Trans.*, **2007**, 364. (b) R. B. King, T. Heine, C. Corminboeuf, P. v. R. Schleyer, *J. Am. Chem. Soc.*, **2004**, *126*, 430.
19. I. B. Bersuker, *Chem. Rev.*, **2001**, *101*, 1067.
20. (a) F. Cimpoesu, K. Hirao, M. Ferbinteanu, Y. Fukuda, W. Linert, *Monatshefte für Chemie*, **2005**, *136*, 1071. (b) F. Cimpoesu, V. Chihaia, N. Stanica, K. Hirao, *Advances In Quantum Chemistry*, **2003**, *44*, 273.
21. (a) I. B. Bersuker, "The Jahn-Teller Effect and Vibronic Interactions in Modern Chemistry", New-York, Plenum Press, 1984. (b) F. Cimpoesu, K. Hirao, "The Ab Initio Analytical Approach of Vibronic Quantities: Application to Inorganic Stereochemistry", *Advances In Quantum Chemistry*, **2003**, *44*, 370.
22. W. Koch, M. C. Holthausen, "A Chemist's Guide to Density Functional Theory", Wiley-VCH, Berlin, **2001**.
23. A. E. Reed, L. A. Curtiss, F. Weinhold, *Chem. Rev.*, **1988**, *88*, 899; the NBO3.0 program, E. D. Glendening, A. E. Reed, J. E. Carpenter, F. Weinhold.
24. NBO 5.0 Glendening E. D., Badenhoop J. K., Reed A. E., Carpenter J. E., Bohmann J. A., Morales C. M., Weinhold F., <http://www.chem.wisc.edu/~nbo>
25. (a) E. D. Glendening, F. Weinhold, *J. Comput. Chem.*, **1998**, *19*, 593; *19*, 610. (b) E. D. Glendening, J. K. Badenhoop, F. Weinhold, *J. Comput. Chem.*, **1998**, *19*, 628. (b) S. Feldgus, C. R. Landis, E. D. Glendening, F. Weinhold, *J. Comput. Chem.*, **2000**, *21*, 11.
26. (a) P. v. R. Schleyer, K. Najafian, "In The Borane, Carborane, Carbocation Continuum", J. Casanova, Ed., Wiley, New York, **1994**. (b) P. v. R. Schleyer, K. Najafian, *Inorg. Chem.*, **1998**, *37*, 3454. (c) M.L. McKee, Z.-X. Wang, P. v. R. Schleyer, *J. Am. Chem. Soc.*, **2000**, *122*, 4781.
27. A. Hirsch, Z. Chen, H. Jiao, *Angew. Chem., Int. Ed.*, **2001**, *40*, 2834.
28. (a) K. Wade, *Adv. Inorg. Chem. Radiochem.*, **1976**, *18*, 1. (b) E. D. Jemmis, M. M. Balakrishnarajan, D. Rabcharatna, *Chem. Rev.*, **2002**, *102*, 93.
29. (a) R. F. W. Bader "Atoms in Molecules - A Quantum Theory", University Press, Oxford, **1990**; (b) R. F. W. Bader, *Acc. Chem. Res.*, **1985**, *18*, 9.
30. F. Biegler-König, "AIM2000" computer code, Bielefeld, **2000**.
31. (a) D. J. Klein, N. Trinajstić (Eds) "Valence Bond Theory and Chemical Structure", Elsevier, Amsterdam, **1990**; (b) D. L. Cooper, J. Gerratt, M. Raimondi, *Chem. Rev.*, **1991**, *91*, 929.

- 
32. M. Ferbinteanu unpublished results.
  33. A. Stasch, M. Ferbinteanu, J. Prust, W. Zheng, F. Cimpoesu, H. W. Roesky, J. Magull, H.-G. Schmidt, M. Noltemeyer, *J. Am. Chem. Soc.*, **2002**, *124*, 5441.
  34. L. Maretti, M. Ferbinteanu, F. Cimpoesu, S. M. Islam, Y. Ohba, T. Kajiwarra, M. Yamashita, S. Yamauchi, *Inorg. Chem.*, **2007**, *46*, 660.
  35. M. J. Frisch, G. W. Trucks, H. B. Schlegel, G. E. Scuseria, M. A. Robb, J. R. Cheeseman, J. A. Montgomery, Jr., T. Vreven, K. N. Kudin, J. C. Burant, J. M. Millam, S. S. Iyengar, J. Tomasi, V. Barone, B. Mennucci, M. Cossi, G. Scalmani, N. Rega, G. A. Petersson, H. Nakatsuji, M. Hada, M. Ehara, K. Toyota, R. Fukuda, J. Hasegawa, M. Ishida, T. Nakajima, Y. Honda, O. Kitao, H. Nakai, M. Klene, X. Li, J. E. Knox, H. P. Hratchian, J. B. Cross, V. Bakken, C. Adamo, J. Jaramillo, R. Gomperts, R. E. Stratmann, O. Yazyev, A. J. Austin, R. Cammi, C. Pomelli, J. W. Ochterski, P. Y. Ayala, K. Morokuma, G. A. Voth, P. Salvador, J. J. Dannenberg, V. G. Zakrzewski, S. Dapprich, A. D. Daniels, M. C. Strain, O. Farkas, D. K. Malick, A. D. Rabuck, K. Raghavachari, J. B. Foresman, J. V. Ortiz, Q. Cui, A. G. Baboul, S. Clifford, J. Cioslowski, B. B. Stefanov, G. Liu, A. Liashenko, P. Piskorz, I. Komaromi, R. L. Martin, D. J. Fox, T. Keith, M. A. Al-Laham, C. Y. Peng, A. Nanayakkara, M. Challacombe, P. M. W. Gill, B. Johnson, W. Chen, M. W. Wong, C. Gonzalez, and J. A. Pople, "*Gaussian 03*", Gaussian, Inc., Wallingford, **2004**.
  36. M. W. Schmidt; K. K. Baldridge; J. A. Boatz, S. T. Elbert, M. S. Gordon, J. H. Jensen, S. Koseki, N. Matsunaga, K. A. Nguyen, S. J. Su, T. L. Windus, M. Dupuis, J. A. Montgomery, *J. Comput. Chem.*, **1993**, *14*, 1347.

